Taavitsainen, Juho; Santos Vilaca da Silva, Pedro; Porter, David; Suikkanen, Pasi

Weldability of Direct-Quenched Steel with a Yield Stress of 960 MPa

Published in:
10th International Conference on Trends in Welding Research and 9th International Welding Symposium of Japan Welding Society (9WS)

Published: 01/01/2017

Weldability of Direct-Quenched Steel with a Yield Stress of 960 MPa

Juho Taavitsainen, Pedro Vilaça
Department of Mechanical Engineering, School of Engineering, Aalto University, Espoo, Finland
juho.taavitsainen@aalto.fi, pedro.vilaca@aalto.fi

David Porter
Materials Eng. and Production Technology, Faculty of Technology, University of Oulu, Oulu, Finland
david.porter@oulu.fi

Pasi Suikkanen
SSAB Europe, POB 93, 92101 Raahe, Finland
pasi.suikkanen@ssab.com

Abstract
The increasingly stringent environmental regulations have raised interest in the use of higher-strength steel, which can enable the design and fabrication of lighter, high-performance structures. Recent innovations in steel processing have made it possible to produce lean alloyed steels with exceptional mechanical properties. As welding is one of the most important manufacturing processes used in industry, the ability to exploit the favourable properties of ultra-high-strength steels is dependent on their weldability. In this work, a commercial, direct-quenched, bainitic-martensitic ultra-high-strength steel with a specified minimum yield stress of 960 MPa, has been studied. The plate thickness was 10 mm and Y-groove butt joints were MAG welded with two passes. The feasibility of using Gleeble specimens to represent specific key-zones of the HAZ was also evaluated. Thus, thermally simulated samples were Charpy impact tested in order to determine the impact transition temperatures of the principal subzones of the heat-affected zone. Hardness measurements and microstructural analyses were used to evaluate the correspondence between the simulated and real heat-affected zones. The relation between the mechanical and metallurgical results on real welds and Gleeble specimens are relevant. A model relating prior austenite grain size and hardness for the CGHAZ was developed and is ready for further exploitation. With low heat input, the 28J transition temperature obtained for the ICCGHAZ was -75.8 °C, revealing a significant improvement from the -29.2 °C obtained for the CGHAZ.

Introduction
Steels are used worldwide and are the most important engineering material for construction and fabrication. Nevertheless the ultra-high strength steels (UHSS), i.e. for tensile strengths exceeding 780 MPa are relatively new to the materials world when compared to the mild steels [1]. As welding is one of the most important manufacturing processes used in industry, the ability to exploit the favourable properties of special steels is dependent on their weldability. Thus, from a manufacturing point of view, the weldability of these steels is of critical importance and represents nowadays a major limitation in the widespread use of the UHSS [2]. Furthermore, the alloying and processing of the steel are the critical factors influencing the microstructures that develop in the heat-affected zone (HAZ) of the welded joints, and hence, the weldability [3]. As a result, there is a strong need to understand the link between the HAZ microstructure and the resulting mechanical properties.

This work addresses the weldability of a modern UHSS. In particular, HAZ properties of a commercial low-alloyed, direct-quenched UHSS [4] with a yield stress of 960 MPa, are investigated. The objective is to investigate the microstructure and mechanical properties that develop in the various subzones of the HAZ in two-run butt welds produced by gas metal arc welding (GMAW). Physical simulation, using the Gleeble thermomechanical simulator, is employed to reproduce samples that can be used for mechanical testing, including impact tests. The purpose of using physical, or thermal, simulation is to enable the reproduction of the HAZ microstructures in quantities that allow characterization of the desired microstructure, which would be difficult, or as in case of impact testing, impossible with samples extracted from the real welds due to the presence of sharp microstructural gradients. Therefore, physical simulation is used for determination of impact transition temperatures. Hardness measurements and microstructural analyses were used to evaluate the correspondence between the simulated and real HAZ. A model relating prior austenite grain size and hardness for the CGHAZ was developed and is evaluated.

Experimental Conditions

Specimens for optical micrography were polished down to 1 μm diamond paste and etched with 2 % nital solution. The optical micrographs were taken from specimens using Nikon Epiphot 200 inverted metallurgical microscope. The microscope was equipped with Nikon DS-U1 digital lenses. For SEM-EBSD, Zeiss Ultra 55 field emission electron microscope (FE-SEM) was used, equipped with Nordlys II EBSD detector by Oxford Instruments. Sample preparation for EBSD was conducted ensuring a deformation-free surface to obtain a sufficiently high diffraction pattern quality.
To measure both prior austenite grain sizes and effective grain sizes on a fine scale, an automated grain size measurement script in Python was implemented according to the mean linear intercept method described in standard ASTM E 1382. To capture and account for any directionality in grain sizes, the measurements are thus done horizontally, vertically and diagonally in rotation increments of 45°. In addition to single-field measurements, a variant of the code capable of measuring grain size gradients along the horizontal direction of a stitched panorama grain boundary image was developed. This was used in determination of the prior austenite grain boundary gradient in the CGHAZ.
Hardness and charpy impact tests were conducted for welded and Gleeble samples. The Gleeble tests were performed using Gleeble 3800 thermomechanical simulator. Gleeble simulations were made to enable a throughout investigation of the three main zones in the HAZ of the welds, namely: Coarse Grain HAZ (CGHAZ); Intercritical HAZ (ICHAZ) and Intercritically reheated CGHAZ (ICCGHAZ). HV1 measurements were performed using a Buehler MMT-7 digital microhardness tester. Charpy impact test were conducted according to standard ISO 148-1. Due to constraints placed by plate thickness and Gleeble test specimens, a reduced-section, i.e. sub-size specimen was used [mm]: 55 x 10 x 5, and test results are fitted using the modified fitting algorithm [5].

The *base material* was an industrial thermomechanically processed and direct-quenched S960 grade steel, with bainitic–martensitic microstructure. The plate thickness was 10 mm. The composition was [wt. %]: 0.092 C; 0.187 Si; 1.10 Mn; 0.01 P; 0.0012 S; 0.033 Al; 0.002 Nb; 0.011 V; 0.014 Cu; 1.14 Cr; 0.398 Ni; 0.0054 N; 0.183 Mo; 0.023 Ti; 0.0017 Ca; 0.0022 B; 0.016 Co. Average grain size was 1.58±1.38 mm (measured from EBSD grain boundary maps using mean linear intercept method and 15° misorientation criterion). The estimated volume fractions of martensite and bainite were 25 % and 75 %, respectively, and in the EBSD maps, no retained austenite was found. Tensile tests were performed according to EN 10149-2 for standard grade S960MC. In longitudinal/rolling direction (RD): yield strength 970 MPa; tensile strength 1123 MPa; elongation 11.6 %. In transverse direction: yield strength 1069 MPa; tensile strength 1192 MPa; elongation 9.8 %. Charpy-V impact toughness tests were performed to get reference properties at low temperatures. Average Cv were as follows for longitudinal direction: 66 J@-20 °C; 54 J@-40 °C; 27 J@-60 °C; and for Longitudinal direction: 109 J@-20 °C; 88 J@-40 °C; 65 J@-60 °C. Thus, in general the requirement of 27 J specified in standard EN 10149-1was clearly overmatched, and only at -60 ℃, for the transverse direction, the value is at the limit.

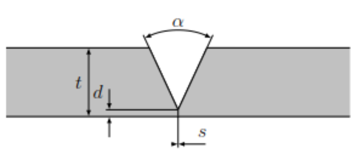

	t (mm)	d (mm)	s (mm)	α (°)
Weld A	10	1	0	45
Weld C	10	1	0	50

a)

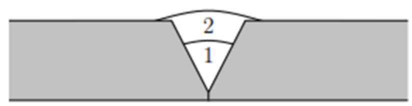

	Run	Polarity	I [A]	E [V]	v_f [m/min]	v [cm/min]	EI/v [kJ/mm]
Weld A	1	DC+	316	26.6	10.6	62.8	0.8
	2	DC+	291	26.5	9.8	57.7	0.8
Weld C	1	DC+	315	26.9	9.9	62.8	0.81
	2	DC+	316	28.8	10.6	36.2	1.51

b)

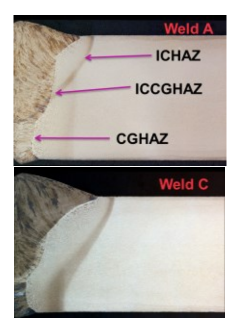

c)

Figure 1: Weld joint design, sequence of weld passes and parameters: a) Weld joint design; b) Welding sequence and parameters; c) Macrograph of the welds with identification of the investigated zones at the HAZ.

The *welding tests* were conducted according to standard ISO 15614-1. The plate dimensions [mm] before welding were 1000 (RD and welding direction) x 200. Two MAG weld samples were produced, designated by "A" and "C" as represented in *Fig. 1*. Both are 2-passes/runs, V-groove butt joint welds, implemented with no air-gap and in flat position without backing. The edge preparation was done by machining. The joint dimensions and weld parameters are depicted in *Fig. 1a* and *1b*. The consumable electrode was Union X 96 with composition [wt. %]: 0.12 C; 0.8 Si; 1.90 Mn; 0.45 Cr; 2.35 Ni; 0.55 Mo (EN 12534). The shielding gas was Ar + 8 % CO_2 + 0.03 % NO. No post-weld treatments were applied to welds. As can be seen by comparing the process parameters in *Fig. 1*b, the welds differ only in the second-run parameters. Second pass of low HI weld “A” corresponds to an estimated cooling time, $t_{8/5}$=4s, and second pass of high HI weld “C” corresponds to an estimated cooling time, $t_{8/5}$=15s.

Analysis of the Results

The hardness measured in the cross section, near the face and root of the 2-passes welds is presented in *Fig. 2*. In general the hardness at the face overmatches 10 to 30 HV the hardness at the root for both weld conditions. The minimum hardness occurs about 3 mm from the fusion line with an undermatching of about 100 HV for weld “A” (low HI) and 130 HV for weld “C” (high HI). The undermatching in the weld metal is about 100 HV for weld “C”, and 50 HV for weld “A”, although at the face, due to highest cooling rate for the 2nd pass with low HI, the hardness of weld metal nearly matches the base material. The extension of the HAZ with hardness undermatching induced by the weld is about 7 mm from fusion line (FL) for the low HI weld “A” and about 12 mm for the high HI weld “C”.

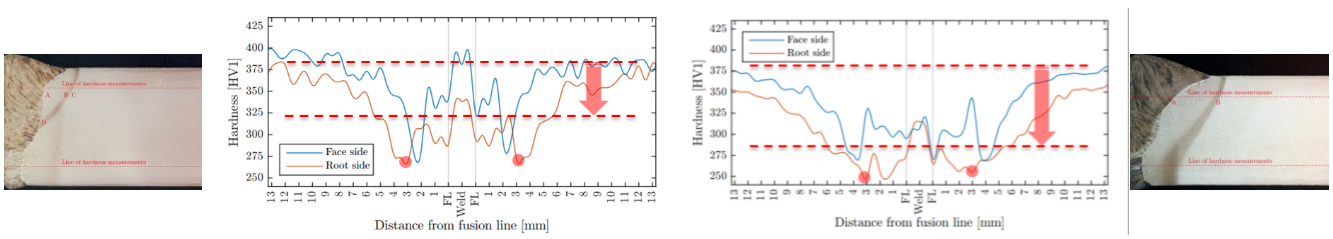

a) b)

Figure 2: Hardness distribution at the face and root sides: a) Low HI weld “A”; a) High HI weld “C”.

The *Fig. 3* presents two microstructures of CGHAZ and ICHAZ of low HI weld and the Charpy-V impact toughness of all the Gleeble simulated samples. Concerning the influence of the HI weld conditions: the increase in HI increased the toughness of the CGHAZ; In opposite effect, the increase in HI decreased the toughness in the ICHAZ and ICCGHAZ. With low heat input, the 28J transition temperature obtained for the ICCGHAZ was -75.8 °C, revealing a significant improvement from the -29.2 °C obtained for the CGHAZ. The Fig. 4 complements the microstructural analysis with the EBSDinverse pole figures of all the different zones and conditions. The CGHAZ microstructure is similar in both samples, with microstructural features reminiscent of bainite and martensite in a relatively coarse prior austenite grain structure. Both ICHAZ shows no texture effects and the one simulating the high HI weld shows the lower grain size. The extent of reaustenitization in ICCGHAZ seems to be significantly lower than what it is observed in the ICHAZ.

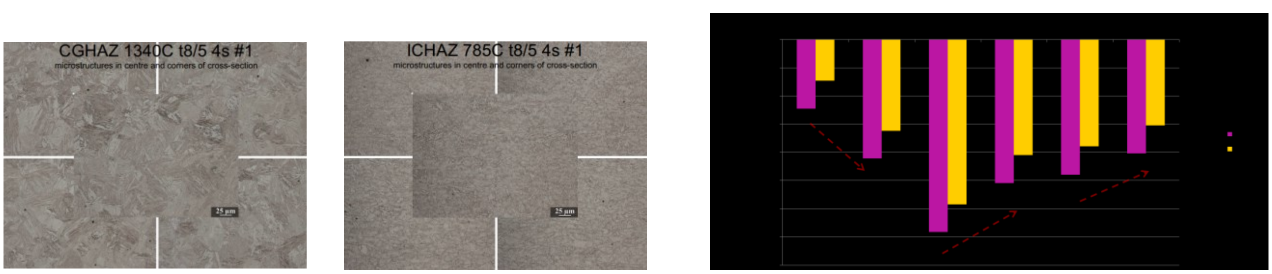

a) b) c)

Figure 3: Results from the Gleeble simulation samples of CGHAZ, ICHAZ, and ICCGHAZ for low HI weld “A” and high HI weld “C”: a) and b) Microstructure of CGHAZ and ICHAZ of low HI weld “A”; c) Charpy-V impact toughness.

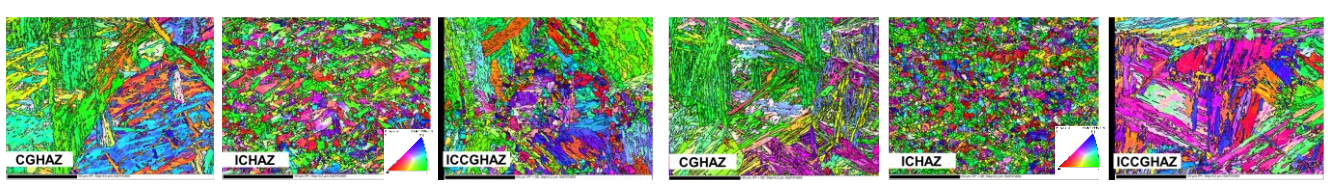

a) b)

Figure 4: SEM/EBSD characterization of Gleeble simulation samples: a) Low HI weld “A”; b) High HI weld “C”.

To investigate the effect of the prior austenite grain size on the hardness of CGHAZ the prior austenite grain size (*Fig. 4*) is correlated with the hardness in *Fig. 5*. A linear regression model is fitted to the data, using the linear least squares method. From the results it can be seen that there is a weak but statistically significant ($p < 0.05$) decreasing trend in the hardness. The findings are in line with literature [6], anyway the existence of a Hall-Petch type relationship between prior austenite grain size in CGHAZ and hardness was tested but it is weak, mainly for the high HI weld "C".

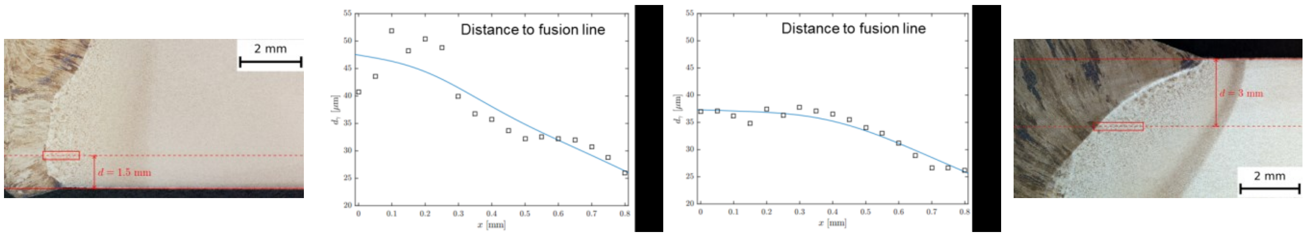

a) b)

Figure 4: Size of prior austenite grain size in CGHAZ of real welds: a) Low HI weld "A"; b) High HI weld "C".

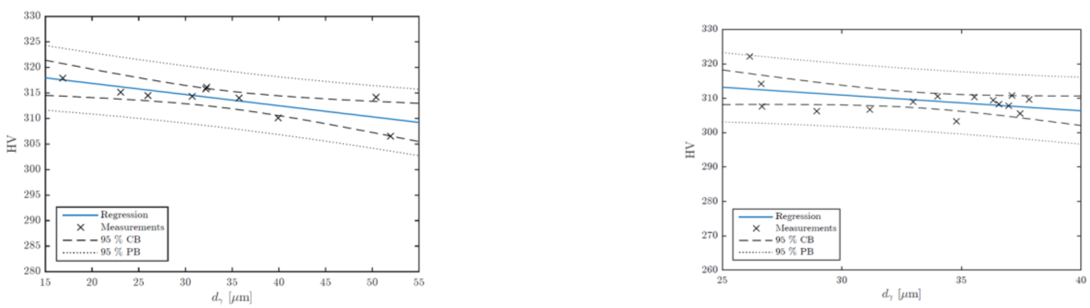

a) b)

Figure 5: Effect of prior austenite grain size, d_γ, on the hardness of CGHAZ: a) Low HI weld "A"; b) High HI weld "C". Note: CB = Confidence bound: uncertainty in slope of regression line; PB = Prediction bound: uncertainty in a single prediction.

Conclusions

Along the weld zone, the hardness near the face (second weld pass) is higher than the hardness near the root for both welds. Minimum hardness occurs about 3 mm from the fusion line with an undermatching of about 100 HV for low HI weld "A" and 130 HV for high HI weld "C". The toughness increases with the increase of HI for the CGHAZ. However, an increase in HI decreased the toughness of the ICHAZ and the ICCGHAZ. The effect on toughness of the ICHAZ thermal cycle is preponderant over the previous CGHAZ. With low HI, the T28J transition temperature obtained for the ICCGHAZ was -75.8 °C, revealing a significant improvement from the -29.2 °C obtained for the CGHAZ. A relationship between the prior austenite grain size in CGHAZ and hardness was tested for both welds, but not found.

References

[1] H. Bhadeshia et al: Steels: microstructure and properties Elsevier Science (2011).
[2] P. Kah, et al: "Welding of ultra-high strength steels". Advanced Materials Research, Vol. 849 (2014) pp. 357–365.
[3] K. Easterling: Introduction to the Physical Metallurgy of Welding, Butterworth-Heinemann (Oxford, 2nd Edition 1992), pp. 126-190.
[4] D. A. Porter: "Developments in hot-rolled high-strength structural steels", *In Nordic Welding Conference*, Tampere, Finland, November, 2006.
[5] K. Wallin. Fracture toughness of engineering materials: estimation and application. EMAS Publishing (Warrington, 2011), pp. 321-372.
[6] S. Morito, et al:. "Effect of block size on the strength of lath martensite in low carbon steels". Materials Science and Engineering: A, Vol. 438 (2006), pp. 237–240.